Conference materials
UDC 54.057
DOI: https://doi.org/10.18721/JPM.183.150

Morphological features of CVD-grown Si nanostructures in meso- and macroporous silicas

D.A. Eurov [1] ✉, V.G. Golubev [1], S.A. Grudinkin [1], D.A. Kurdyukov [1],
D.A. Kirilenko [1], A.A. Yakovleva [1], E.Yu. Stovpiaga [1]

[1] Ioffe Institute, St. Petersburg, Russia
✉ post@mail.ioffe.ru

Abstract. Morphology of silicon nanostructures obtained by thermal chemical vapour deposition (CVD) method in mesoporous silica particles ($mSiO_2$) and macroporous synthetic opal were studied. The proposed method allows obtaining a uniform Si layer on the surface of non-porous spherical silica particles forming macropores in opal, in contrary, to complete filling of 3-nm pores inside mesoporous particles with amorphous silicon. The thermal CVD provides for gradual change of pore filling which, in turn, leads to step-to-step variation of porosity characteristics in the case of $mSiO_2$/Si and the modification of photonic crystal properties in the case of opal-Si.

Keywords: spherical particles, silicon, nanostructures, silica, mesopores, opal

Funding: This work was funded by the Russian Science Foundation, project No. 23-79-00018.

Citation: Eurov D.A., Golubev V.G., Grudinkin S.A., Kurdyukov D.A., Kirilenko D.A., Yakovleva A.A., Stovpiaga E.Yu., Morphological features of CVD-grown Si nanostructures in meso- and macroporous silicas, St. Petersburg State Polytechnical University Journal. Physics and Mathematics. 18 (3.1) (2025) 252–257. DOI: https://doi.org/10.18721/JPM.183.150

Материалы конференции
УДК 54.057
DOI: https://doi.org/10.18721/JPM.183.150

Особенности морфологии Si наноструктур, выращенных в мезо- и макропористых кремнеземах методом CVD

Д.А. Еуров [1] ✉, В.Г. Голубев [1], С.А. Грудинкин [1], Д.А. Курдюков [1],
Д.А. Кириленко [1], А.А. Яковлева [1], Е.Ю. Стовпяга [1]

[1] Физико-технический институт им. А.Ф. Иоффе РАН, Санкт-Петербург, Россия
✉ post@mail.ioffe.ru

Аннотация. Изучена морфология кремниевых наноструктур, получаемых методом термического газофазного осаждения, внутри частиц мезопористого кремнезема ($mSiO_2$) и коллоидного кристалла – макропористого синтетического опала. Предложенный метод позволяет получить однородный слой Si на поверхности непористых сферических частиц кремнезема, образующих макропоры в опале, тогда как 3-нм поры внутри мезопористых частиц полностью заполняются аморфным кремнием. Применяемый технологический подход обеспечивает постепенное изменение степени заполнения пор, в свою очередь, определяющее ступенчатое изменение характеристик пористости $mSiO_2$/Si и модификацию фотонно-кристаллических свойств композита опал-Si.

Ключевые слова: сферические частицы, кремний, наноструктуры, кремнезем, мезопоры, опал

Финансирование: Работа выполнена за счет гранта Российского научного фонда № 23-79-00018.

Ссылка при цитировании: Еуров Д.А., Голубев В.Г., Грудинкин С.А., Курдюков Д.А., Кириленко Д.А., Яковлева А.А., Стовпяга Е.Ю. Особенности морфологии Si наноструктур, выращенных в мезо- и макропористых кремнеземах методом CVD // Научно-технические ведомости СПбГПУ. Физико-математические науки. 2025. Т. 18. № 3.1. С. 252–257. DOI: https://doi.org/10.18721/JPM.183.150

Introduction

There has been rapidly increasing interest in design and synthesis of silicon-based nanostructured materials for photonics, photovoltaics and bioapplications [1, 2]. Silicon nanocrystals, nanowires and photonic crystals are key examples of functional nanostructures with properties determined by their morphology [1, 2]. One of the ways to tailor the morphology of nanostructures is the use of porous template approach [3, 4]. The pore size and shape of the template are the main characteristics which determine the morphological features and thus the structural parameters of the silicon nanostructures formed. The goal of this work was to study the difference in morphology of silicon nanostructures grown by thermal chemical vapor deposition (CVD) method in two kind of silica templates: mesoporous particles and macroporous synthetic opals. The variation of porosity characteristics and the modification of opal-Si photonic crystal properties were demonstrated.

Materials and Methods

Materials. We used the following reagents: cetyltrimethylammonium bromide (CTAB, $C_{16}H_{33}N(CH_3)_3Br$), 99.99% (Acros Organics); aqueous ammonia (NH_3), 24 wt%; ethanol (C_2H_5OH), 95.7 vol%; deionized water (H_2O) with a resistance of 10 MΩ; tetraethoxysilane (TEOS, $Si(OC_2H_5)_4$), 99.9% (Acros Organics); monosilane (SiH_4), electronic grade (Sigma-Aldrich); argon (Ar), 99.998% (Sigma-Aldrich). All the chemicals were of analytical purity grade commercially available. There was no need to additionally purify the reagents.

Methods. The silica particles, opals and SiO_2/Si composites were obtained based on our previously developed methods. In particular, the procedure for the synthesis of non-porous spherical silica particles ($nSiO_2$) with a diameter of 740 ± 30 was similar to that employed in [5, 6] via hydrolysis of TEOS in a mixture NH_3–H_2O–C_2H_5OH. Spherical mesoporous silica particles ($mSiO_2$) with a diameter of 385 ± 20 nm and a pore diameter of 3.1 ± 0.15 nm were synthesized according to the method developed by us via basic hydrolysis of TEOS in NH_3–H_2O–C_2H_5OH–CTAB mixture [7, 8]. The opal films were grown from close-packed $nSiO_2$ particles on substrates made from optically polished microscope glass by using the vertical deposition technique as described in [9, 10]. The volume available for filling was up to 26% of the total opal volume, and the interparticle macropore size was 100–300 nm. For the synthesis of silicon within the pores of opal and $mSiO_2$ particles we used the modified method of monosilane thermal decomposition at 450 °C during 0–60 h [11, 12].

Transmission electron microscopic (TEM) measurements were performed using a Jeol JEM-2100F microscope (accelerating voltage 200 kV, point-to-point resolution 0.19 nm) equipped with Bruker XFlash 6T-30 energy dispersive X-ray (EDX) spectrometer. The nitrogen adsorption was performed using a Micromeritics 3FLEX at a temperature of 77 K. The specific surface area was calculated by the Brunauer – Emmett – Teller (BET) method, and the pore size distribution was found using the nonlocal density functional theory (NLDFT). The optical transmission spectra were measured by a Bruker IFS 113v Fourier spectrometer in the near infrared region. The spectra were registered by using a cooled InSb detector and a halogen lamp as a light source. The spectral resolution was 4 cm^{-1}. The incident light was focused onto the sample within the solid angle of 10°.

Results and Discussion

We used different porous silicas, namely, spherical $mSiO_2$ particles with 3-nm cylindrical mesopores and silica colloidal crystals (synthetic opals) with interparticle macropore size of 100–300 nm. The thermal destruction of SiH_4 occurs uniformly within the whole pore volume of the templates because in the thermal CVD method we developed, the limiting stage of the process in which pores are filled with silicon is the reaction in which monosilane is decomposed, rather than its diffusion within template pores [11, 12]. According to X-ray diffraction and Raman measurements, silicon formed in the macro- and mesopores is amorphous.

Fig. 1, *a* shows the isotherms for the $mSiO_2$ particles as the mesopores are filled with silicon due to thermal decomposition of SiH_4. It can be seen, that for particles that were filled with Si for up to 45 hours, the shape of the isotherms does not change. The NLDFT pore size distribution (Fig. 1, *b*) indicates the presence of only one pronounced peak at 3.1 nm, which corresponds to the size of CTAB micelles. Apparently, inside the $mSiO_2$ particles, there is a complete filling of the mesopores with silicon (Fig. 1, *c*, inset). Probably, the near-surface pores are filled first, then, gradually, as the duration of the process increases, the boundary between the regions of filled and unfilled pores shifts deeper inside the particles. Access of SiH_4 into the volume of particles preserves since they possess the branched interconnected structure of pores. When the pore

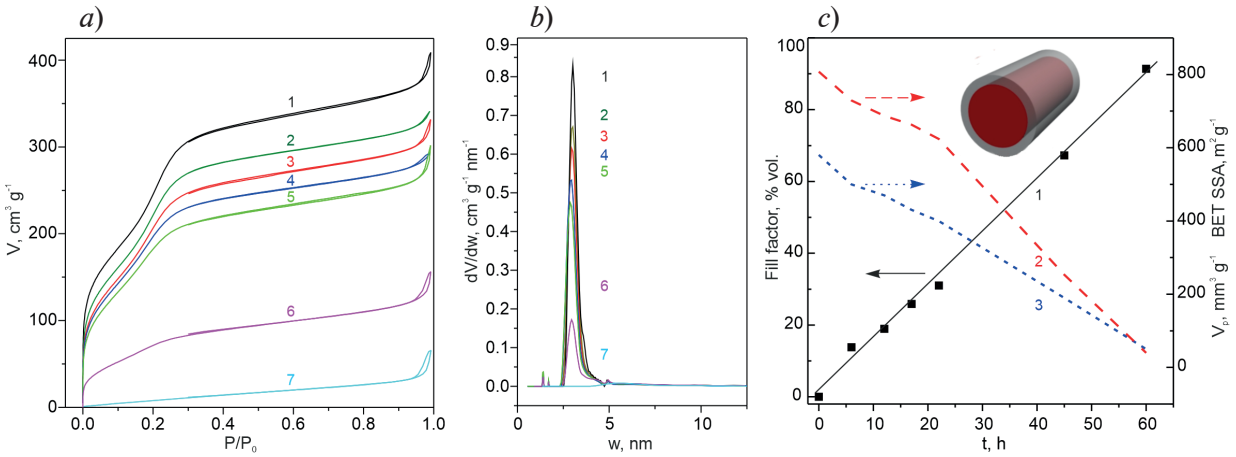

Fig. 1. N_2 adsorption and desorption isotherms measured at 77 K (*a*) and NLDFT pore size distributions (*b*) for the mesoporous silica particles filled with silicon. Filling duration (h): 1 – 0, 2 – 6, 3 – 12, 4 – 17, 5 – 22, 6 – 45, 7 – 60. (*c*) Dependence of pore fill factor (*1*), specific surface area (*2*) and free pore volume (*3*) of $mSiO_2$/Si particles on filling duration. Inset shows a schematic of filled pore

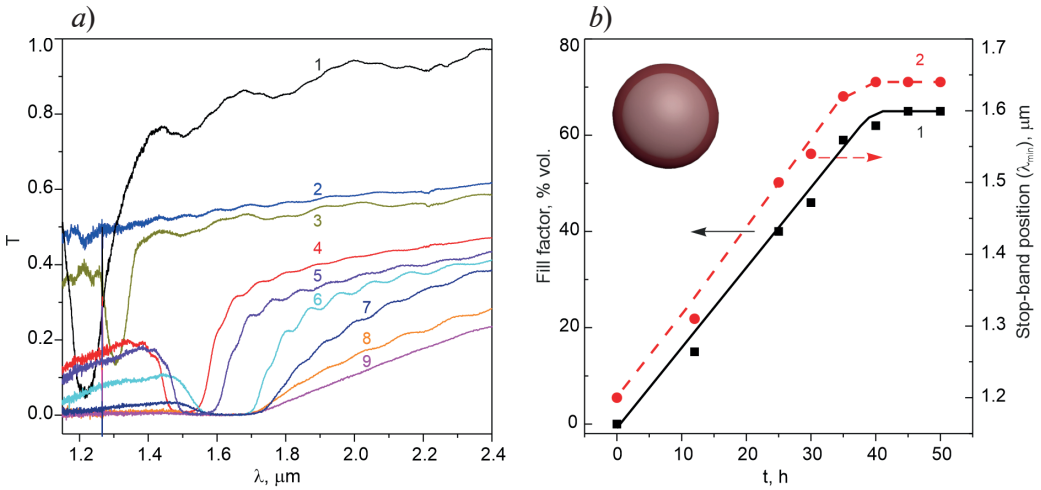

Fig. 2. (*a*) Transmission spectra of the opal/Si composite on a glass substrate. Filling duration (h): 1 – 0, 2 – 6, 3 – 12, 4 – 25, 5 – 30, 6 – 35, 7 – 40, 8 – 45, 9 – 50. (*b*) Dependence of pore fill factor (*1*), and photonic stop-band position (*2*) of opal/Si on filling duration. Inset shows a schematic of a non-porous particle covered with Si layer

filling is close to complete (Fig. 1, *a*, *b*, curve *7*), the 3-nm pores disappear and larger pores are recorded, which are apparently interparticle pores. The SSA values calculated by BET method (BET SSA) and pore volumes decrease monotonically as filling time increases (Fig. 1, *c*). The pore filling degree was calculated based on the change in free pore volume. The TEM images of $mSiO_2$/Si composite particles (Fig. 3, *a*) show that the particle contrast is uniform, indicating uniform filling of the particles with silicon without any unfilled regions. Note, that there is no silicon layer on the outer surface of the particles, thus the developed technique allows selective filling of mesopores.

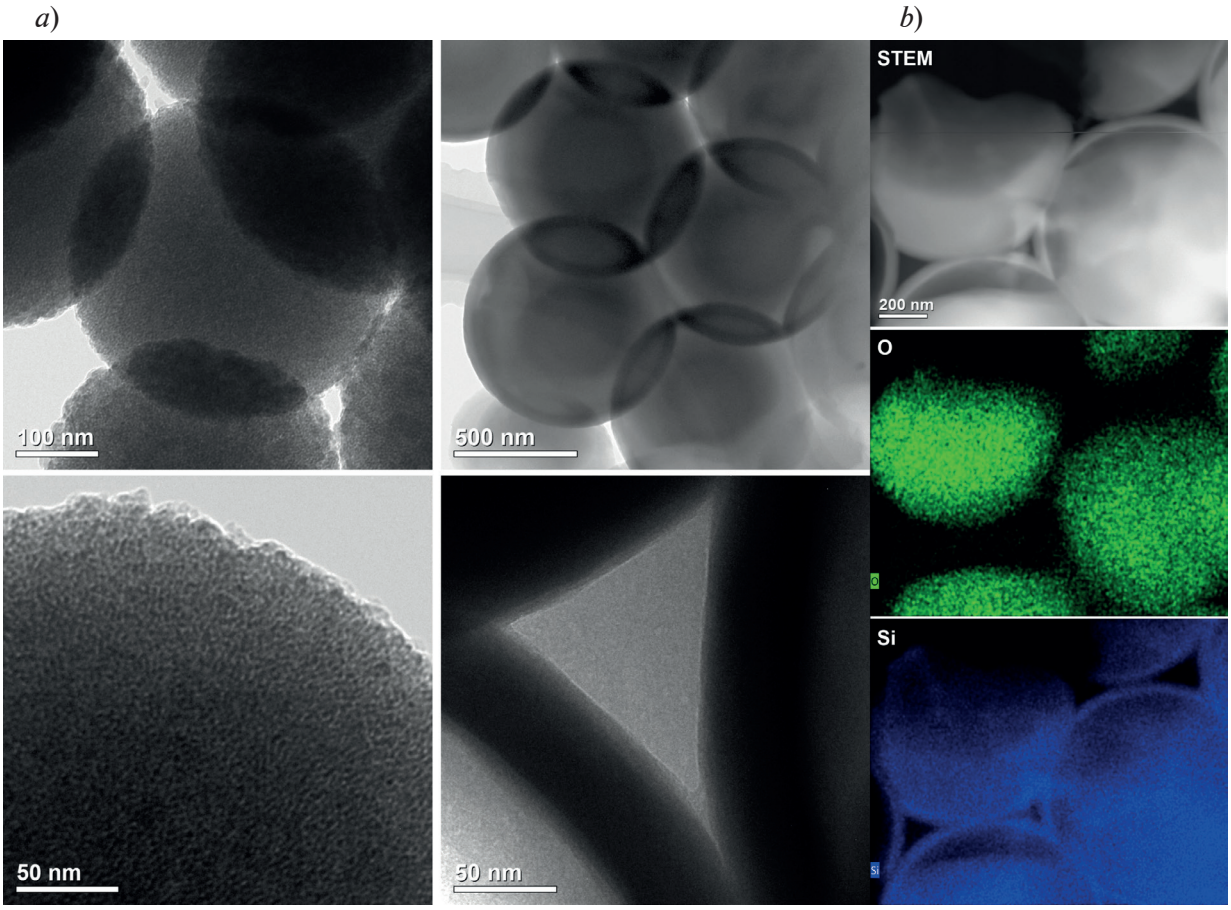

Fig. 3. TEM and STEM images for the $mSiO_2$/Si (*a*) and opal/Si (*b*) and EDX elemental maps for opal/Si (*b*)

An essential feature of the opal/Si composite obtained is the manifestation of typical properties of photonic crystals [10, 13]. We could control and estimate the filling degree from the stop-band (dip) position in the transmission spectra caused by Bragg diffraction from the (111) planes of the f.c.c. lattice of the composite (Fig. 2, *a*). The position of the extremum of the diffraction line λ_{111} at normal incidence can be described by Bragg's formula $\lambda_{111} = 2d_{(111)}\sqrt{\langle\varepsilon\rangle}$, where $d_{(111)}$ is the interplane distance, $\langle\varepsilon\rangle$ is the average dielectric constant of the composite, and $\langle\varepsilon\rangle = \sum \varepsilon_i f_i$ (ε_i and f_i are the dielectric constant and the volume fraction of the *i*-th constituent, respectively [10]). The dielectric constant of the SiO_2 spheres and a-Si were taken to be 1.96 [10], and 13.7, correspondingly. There is no stop-band in curve 2 in Fig. 2, *a* due to the absence of optical contrast when the alignment of the average dielectric constants of spherical particles and the pore space occurs. In addition to the Bragg diffraction line, the transmission spectra contained interference fringes due to light reflection from two plane-parallel film surfaces.

Fig. 2, *b* shows that in the opal film, which was filled with Si for up to 40 hours, the position of the stop-band and the corresponding value of the pore fill factor change linearly with the change in the duration of the filling process. Then, the dependencies reach saturation, probably due to

the fact that the narrowest areas of the pores are completely filled with silicon. Unlike mesoporous particles, in opal the complete filling of the pores is not achieved, the maximum degree of filling is ~65%.

Fig. 3, *b* shows TEM images and EDX elemental maps for the obtained opal/Si composite. The boundaries of the $nSiO_2$ particles forming opal structure and silicon shell are clearly distinguishable. It can be seen that, unlike the mesoporous template, in opal the process of layer-by-layer coating of the surface of silica particles with silicon is realized (Fig. 2, *b*, inset) and the thickness of the layer can be controllably varied, which follows from the smooth change in the photonic crystal properties of the composite (Fig. 2).

Conclusion

An approach for the gradual variation of fill factor of both meso- and macroporous silicas with amorphous silicon by use of thermal CVD technique is proposed. The synthesis of a-Si is carried out by thermal decomposition of monosilane within the pores of the templates. It is shown that the fill factor changes lead to step-to-step variation of porosity characteristics and the modification of opal-Si photonic crystal properties. It is found that in the opal template the formation of uniform layer of the same thickness on each SiO_2 particle occurs, in contrast, the complete filling of 3-nm pores inside mesoporous particles with amorphous silicon takes place. The developed technique is a promising tool for obtaining functional particles for biomedical applications and active optical media on the base of synthetic opals.

Acknowledgments

The TEM study was carried out on equipment of the Federal Joint Research Center “Material science and characterization in advanced technology”.

REFERENCES

1. **He Y., Fan C., Lee S.-T.,** Silicon nanostructures for bioapplications, Nanotoday. 5 (2010) 282–295.

2. **Priolo F., Gregorkiewicz T., Galli M., Krauss T.F.,** Silicon nanostructures for photonics and photovoltaics. Nature Nanotechnology. 9 (2014) 19–32.

3. **Martin C.R.,** Nanomaterials: a membrane-based synthetic approach, Science. 266 (1994) 1961–1966.

4. **Colilla M., González B., Vallet-Regi M.,** Mesoporous silica nanoparticles for the design of smart delivery nanodevices. Biomaterial Science. 1 (2013) 114–134.

5. **Stöber W., Fink A., Bohn E.,** Controlled growth of monodisperse silica spheres in the micron size range, Journal of Colloid and Interface Science. 26 (1) (1968) 62–69.

6. **Trofimova E.Yu., Aleksenskii, A.E., Grudinkin S.A., Korkin I.V., Kurdyukov D.A., Golubev V.G.,** Effect of tetraethoxysilane pretreatment on synthesis of colloidal particles of amorphous silicon dioxide, Colloid Journal. 73 (2011) 546–550.

7. **Trofimova E.Yu., Kurdyukov D.A., Yakovlev S.A., Kirilenko D.A., Kukushkina Yu.A., Nashchekin A.V., Sitnikova A.A., Yagovkina M.A., Golubev V.G.,** Monodisperse spherical mesoporous silica particles: fast synthesis procedure and fabrication of photonic crystal films, Nanotechnology. 24 (2013) 155601.

8. **Eurov D.A., Kurdyukov D.A., Medvedev A.V., Kirilenko D.A., Tomkovich M.V., Golubev V.G.,** Micro-mesoporous submicron silica particles with pore size tunable in a wide range: synthesis, properties and prospects for LED manufacturing, Nanotechnology. 32 (2021) 215604.

9. **Jiang P., Bertone J.F., Hwang K.S.,** Colvin V.L., Single-crystal colloidal multilayers of controlled thickness, Chemistry of Materials. 11 (1999) 2132–2140.

10. **Grudinkin S.A., Kaplan S.F., Kartenko N.F., Kurdyukov D.A., Golubev V.G.,** Opal-hematite and opal-magnetite films: lateral infiltration, thermodynamically driven synthesis, photonic crystal properties. Journal of Physical Chemistry C. 112 (2008) 17855–17861.

11. **Bogomolov V.N., Golubev V.G., Kartenko N.F., Kurdyukov D.A., Pevtsov A.B., Prokof'ev A.V., Ratnikov V.V., Feoktistov N.A., Sharenkova N.V.,** Fabrication of regular three-dimensional lattices of submicron silicon clusters in an SiO_2 opal matrix. Technical Physics Letters. 24 (2017) 326–327.

12. **Kurdyukov D.A., Eurov D.A., Shmakov S.V., Kirilenko D.A., Kukushkina J.A., Smirnov A.N., Yagovkina M.A., Klimenko V.V., Koniakhin S.V., Golubev V.G.,** Fabrication of doxorubicin-loaded monodisperse spherical micro-mesoporous silicon particles for enhanced inhibition of cancer cell proliferation, Microporous Mesoporous Mater. 281 (2019) 1–8.

13. **López C.,** Materials aspects of photonic crystals, Advanced Materials. 15 (2003) 1679–1704.

THE AUTHORS

EUROV Daniil A.
edan@mail.ru
ORCID: 000-0002-7471-4028

GOLUBEV Valery G.
golubev@gvg.ioffe.ru
ORCID: 0000-0003-2956-6561

GRUDINKIN Sergey A.
grudink@gvg.ioffe.ru
ORCID: 0000-0003-1344-9483

KURDYUKOV Dmitry A.
kurd@gvg.ioffe.ru
ORCID: 0000-0002-3041-9609

KIRILENKO Demid A.
zumsisai@gmail.com
ORCID: 0000-0002-1571-209X

YAKOVLEVA Anastasiia A.
nastama@mail.ru
ORCID: 0000-0003-0651-6860

STOVPIAGA Ekaterina Yu.
kattrof@gvg.ioffe.ru
ORCID: 0000-0003-0434-5252

Received 14.08.2025. Approved after reviewing 09.09.2025. Accepted 10.09.2025.